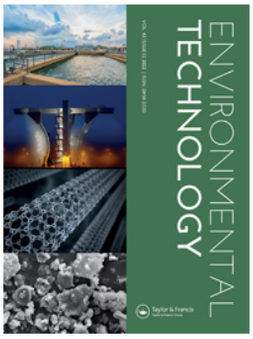

Environmental Technology

ISSN: (Print) (Online) Journal homepage: https://www.tandfonline.com/loi/tent20

Fenton pre-oxidation of natural organic matter in drinking water treatment through the application of iron nails

Naiara de O. dos Santos, Luiz A. Teixeira, Qizhi Zhou, Grace Burke & Luiza C. Campos

To cite this article: Naiara de O. dos Santos, Luiz A. Teixeira, Qizhi Zhou, Grace Burke & Luiza C. Campos (2021): Fenton pre-oxidation of natural organic matter in drinking water treatment through the application of iron nails, Environmental Technology, DOI: 10.1080/09593330.2021.1890838

To link to this article: https://doi.org/10.1080/09593330.2021.1890838

ENVIRONMENTAL TECHNOLOGY
https://doi.org/10.1080/09593330.2021.1890838

Fenton pre-oxidation of natural organic matter in drinking water treatment through the application of iron nails

Naiara de O. dos Santos[a,c], Luiz A. Teixeira[a,b], Qizhi Zhou[c], Grace Burke[d] and Luiza C. Campos [c]

[a]Department of Chemical and Materials Engineering, PUC-Rio, Rio de Janeiro, Brazil; [b]Peroxidos do Brasil Ltda – Solvay Group; [c]Department of Civil, Environmental and Geomatic Engineering, University College London, London, UK; [d]Materials Performance Centre, School of Materials, The University of Manchester, Manchester, UK

ABSTRACT

This study investigated for the first time the efficiency of an advanced oxidation process (AOP) zero valent iron/hydrogen peroxide (ZVI/H_2O_2) employing iron nails for the removal of Natural Organic Matter (NOM) from natural water of Regent's Park lake, London, UK. The low cost of nails and their easy separation from the water after the treatment make this AOP attractive for water utilities in low- and middle-income countries. The process was investigated as a pre-oxidation step for drinking water treatment. Results showed that UV254 removal in the natural water was lower than that of simulated water containing commercial humic acid (HA), indicating a matrix effect. Statistical analysis confirmed the maximum removal of dissolved organic carbon (DOC) in natural water depends on the initial pH (best at 4.5) and H_2O_2 dosage (best at 100% excess of stoichiometric dosage). DOC and UV254 removals under this operational condition were 51% and 89%, respectively. Molecular weight (MW) and specific UV absorbance (SUVA254) were significantly reduced to 74% and 78%, respectively. Formation of Chloroform THM in natural water sample after the ZVI/H_2O_2 process (initial pH 4.5) was below the limit for drinking water, and 48% less than the THM formation in the same water not subjected to pre-oxidation. Characterization of oxidation products on the iron-nail-ZVI surface after the ZVI/H_2O_2 treatment by SEM, XRD, and XPS identified the formation of magnetite and lepidocrocite. Results suggest that the investigated ZVI/H_2O_2 process is a promising technology for removing NOM and reducing THM formation during drinking water treatment.

ARTICLE HISTORY
Received 17 November 2020
Accepted 8 February 2021

KEYWORDS
Natural organic substances; natural water; pre-oxidation; ZVI-Fenton; THM

Introduction

Surface waters in various regions contain natural organic matter (NOM) with a significant percentage of humic acids (HA) [1]. These are known precursors in the formation of disinfection by products (DBPs), in particular toxic chlorinated organics produced by the reaction with chlorine during drinking water treatment [2,3].

Amongst the halogenated DBPs, trihalomethanes (THMs) are the ones found in higher concentrations in drinking water [4,5]. These are associated with increased risk of cancer, especially in the bladder, and adverse reproductive outcomes [6]. Making the situation worse in WTPs, the application of pre-chlorination for taste/odour or iron/manganese control prior to coagulation can increase the generation of a variety of DBPs [7]. In addition, in conventional water treatment trains, the steps of coagulation and flocculation followed by sedimentation or flotation, and filtration are only partially effective at removing NOM [8,9].

In this context, due to the need for improving existing treatments, alternative processes for NOM have been proposed. Some of these processes include: activated carbon filtration/adsorption [10], membrane filtration [11–13] and advanced oxidation processes (AOPs) [9,14,15].

AOPs are the WTP technologies that have attracted most interest in the last two decades because of their potential to reduce the formation of DBPs [3,16]. AOPs are generally applied for commercial drinking water under low to moderate oxidation conditions. Even in these operating conditions, NOM with higher molecular weight compounds is partially oxidized and transformed into smaller ones, such as aldehydes and carboxylic acids, which are more biodegradable molecules [17,18]. These chemical modifications can result in the overall decrease of Total Organic Carbon (TOC) and Disinfection Byproduct Formation Potentials (DBPFP) in the treated water [17,19]. And among the AOPs, the Fenton process has already been proposed to optimize the removal of

CONTACT Luiza C. Campos l.campos@ucl.ac.uk Department of Civil, Environmental and Geomatic Engineering, University College London, London, WC1E 6BT, UK

Supplemental data for this article can be accessed https://doi.org/10.1080/09593330.2021.1890838

several organic contaminants from waters [8,20–23]. This process utilizes hydrogen peroxide (H_2O_2) and soluble iron (II) salts to produce a highly reactive radical (HO•) capable of oxidizing organic compounds in solution. Previous Fenton studies (photo-Fenton and Electro-Fenton) were reported to potentially remove organics with a wide molecular weight range from the humic acid structure, achieving the fragmentation of hydrophobic fractions into hydrophilic fractions [24,25]. In recent years, alternatives to soluble iron salts in the Fenton process have been investigated, mainly aimed at the use of solid elemental iron (Fe^0/ZVI) as this is an efficient electron donor [26,27]. However, the disadvantages of removing metalic iron in the form of particulate powder during and at the end of the treatment have driven interest to a search for other forms of ZVI [27–36] which may allow easier separation from the water. Among these studies, similar rates of TOC removal have been reported when using ZVI in less conventional forms (such as metal shavings) compared to commercial particulate ZVI powder [36].

This strategy of employing low-cost commercially available ZVI materials can be attractive for the application of the Fenton (ZVI/H_2O_2) process [27], mainly for municipalities that may lack financial resources to afford advanced water treatment processes with complex equipment such as ozone generators or UV photo-reactors. For example, the cost of ZVI powder with 97%–99% of purity range from 60 to 150.0 $ USD/Kg [37], while the cost of commercial iron-nails range from 1.0 to 3.0 $ USD/Kg. Considering this, some researchers have applied commercial iron-nails in different water/wastewater treatments e.g. in sand filters during the filtration process for arsenic removal [38–41], in Electrocoagulation process for removal of mercury (II) [42], and in ultrasound-assisted Fenton process for wastewater treatment [43]. However, the application of commercial iron-nails for NOM removal in the drinking water treatment plants has not been reported. Therefore, the main purpose of the present work was to investigate the removal of NOM in natural surface water using commercial iron-nails in the ZVI/H_2O_2 process as a pre-oxidation step to conventional WTPs. To the authors' knowledge, this is the first study applying ZVI in the form of iron-nails to the ZVI/H_2O_2 process to remove NOM and reduce THM formation during drinking water treatment.

2. Materials and methods

2.1. Materials and chemicals

Commercial HA (Sigma-Aldrich), hydrogen peroxide (50% w/w) (Solvay Group), THM standards (Supelco; purity of 99.9%), sodium polystyrene sulfonates (PSS, Polymer Standards Service GmbH, Germany), methyl-tertiary-butyl-ether (MtBE) (Sigma-Aldrich), sodium sulfite (Merck;purity of 99%), and all other chemical reagents were of analytical grade and the solutions were prepared with ultrapure water (Millipore Milli-Q, resistivity > 18.2 MΩ.cm). The ZVI nail was obtained in the form of small low-carbon-steel nails (AISI 1010) with 0.43 cm^2 g^{-1} (surface area per gram of each nail). The chemical composition (mass concentration – %) performed by optical emission spectroscopy – OES (Spectromax Instrument) confirmed that the total trace elements content in the nail is less than 1%, as shown in Table A.1.

Natural water samples were collected from the Regent's Park lake (London, UK – 51°31′28″ N 0°09′15″ W) (Figure A.1) in 1-L bottles for each sample, during August and September 2018.

2.2. Preparation of samples

Simulated water was prepared by dissolving 0.01 g of commercial HA in 15 mL of 0.1 M NaOH solution [20] and was homogenized on a shaker (175 rpm) for ± 14 h to fully dissolve. Hydrogen peroxide was used to prepare a 1.0 g L^{-1} stock solution.

The stoichiometric H_2O_2 dosage applied to the simulated water containing HA and natural water was 8.6 mg L^{-1} per mg L^{-1} of dissolved organic carbon (DOC) [44,45]. Stoichiometric dosages of sodium sulfite [46] were added to the samples at the end of ZVI/H_2O_2 experiments to extinguish the remaining concentrations of H_2O_2 and to prevent the influence of sodium sulfite excesses on the chlorine extinction at the chlorination step. The pH of the samples subjected to the ZVI/H_2O_2 process was adjusted to pH 7.0 at the end of each run, before the chlorination step.

Preliminary chlorine demand tests on water samples collected from Regent's Park indicated that a chlorine dosage of 4.0 mg L^{-1} was required for providing a residual concentration of free chlorine of 0.5 ± 0.15 mg L^{-1} [47]. After the ZVI/H_2O_2 process, samples were subjected to 30 min and 24 h of contact time (Ct) with chlorine (4.0 mg L^{-1}) [48,49]. The sodium sulfite was added at the end of each contact time to extinguish the remaining concentrations of chlorine. After the chlorination step, the samples were stored according to USEPA Method 551.1 [50] for later analysis of THM formation. THM standards were prepared by dissolving in methanol, at 2000 µg mL^{-1} each.

2.3 Analytical procedures

The UV_{254} (Shimadzu UV 1800 spectrophotometer), DOC (TOC-L CPH model TOC analyser) and specific UV

absorbance [SUVA (L mg^{-1} m^{-1}) = UV_{254}/DOC * 100] determinations were obtained according to USEPA Method 415.3 [51] and Standard Methods 5910B [52]. For molecular weight (MW) analysis, a calibration was performed using a set of four sodium polystyrene sulfonates (PSS, Polymer Standards Service GmbH, Germany) together with Acetone ($R^2 = 0.998$). Of the various standards available for MW measurement, PSS have been widely applied [53–60] as they are more similar to NOM with regards to charge density [53,54]. After the calibration step, a semi-logarithmic linear calibration curve was obtained and used to determine the MW. These calibration curves were constructed by determining the peak retention times of the patterns with narrow MW distribution, following methodologies and equations by Liu and Fitzpatrick [53] and Zhou et al. [54]. The MW values of NOM before and after the ZVI/H_2O_2 reaction were determined by high pressure size exclusion chromatography (HPSEC) on the HPLC system (Perkin Elmer, UK) equipped with a 200 series pump, autosampler and 254 nm UV detector, following Liu and Fitzpatrick's methodology [53]. The analyses of total THM were performed by gas chromatography (GC) (Claurus 500 model) with column (Restek Rxi-5ms, 30 m × 0.25 mm ID) coupled with mass spectrometry (MS) by liquid/liquid extraction with methyl-tertiary-butyl-ether (MtBE), following USEPA Method 551.1 [50] and Rasheed et al. [61]. GC analytical conditions are given in Table A.2. The H_2O_2 concentration was monitored according to Solvay-Peroxidos Brasil's method [62] on a HACH 890 colorimeter at 420 nm (detection interval 0.1–10.0 mg L^{-1}). The determination is based on the reaction between H_2O_2 and a titanium (IV) salt in an aqueous acidic solution to produce a yellow complex of perititanic acid.

The surface morphology of the ZVI nail was analysed using scanning electron microscope (SEM) (FEG, 'Field Emission Gun') (Zeiss Merlin, and Zeiss Ultra 55) in both secondary electrons (SE) and backscattered electrons (BSE) imaging modes. The operating voltage for imaging ranged from 1.5 to 5 kV. X-ray energy dispersive spectroscopy (XEDS) provided qualitative compositional information about the surface deposits on the ZVI nail. XEDS elemental maps were acquired using the Zeiss Merlin FEG–SEM equipped with an Oxford Instruments low voltage X-Max Extreme 100 windowless silicon drift detector (SDD). All XEDS data were collected with incident electron beam energy in the range of 1.5–3 kV, which significantly reduces the volume of the specimen that generates the XED spectra; thus, it was possible to obtain qualitative compositional data from a surface/near surface region of ∼ 20–50 nm in depth. The oxides species on the ZVI nail surface after ZVI/H_2O_2 reaction were identified by X-ray diffraction (XRD) using Proto AXRD system diffractometer θ–2θ diffractometer (284 mm diameter) and X-ray photoelectron spectroscopy (XPS) using spectrometer Thermo K-alpha (E = 1486.6 eV). The dissolved Fe^{2+} formed during the experiments was measured at the time of aliquoting after filtering the samples in a 0.45 µm membrane filter. The analyses were performed on a HACH 890 colorimeter at 520 nm (10-phenanthroline method adapted from Standard Methods for the Examination of Water and Wastewater) [63–65].

2.4 Experimental procedure

Prior to the start of the experiments, the ZVI nail was subjected to a chemical cleaning/pickling step (by immersion in 1% HCl solution for 10 min) and was washed three times with distilled water after the pickling to remove any surface dirt and remaining acid. ZVI/H_2O_2 runs were conducted following a statistical factorial design – 2^3. All experiments were performed in 1-L beakers under agitation at 250 rpm in Jar-test equipment (temperature 23 ± 1°C). The pH of the solution was initially adjusted to the set initial value with H_2SO_4 (0.01 M) and the required H_2O_2 dosage was injected into the solution. The pH stability was verified for the possible need for re-adjustment, and then the ZVI was added triggering the start of the reaction. The aliquots were previously filtered through a 0.45 µm membrane filter (Millipore) and analyses of Fe^{2+}, residual H_2O_2, and pH were performed immediately. In the respective times of taking the aliquots, the oxidation reaction by H_2O_2 was extinguished with sodium sulfite (except for H_2O_2 measuring). The remaining samples were stored under refrigeration (4° C) for further analysis.

2.5 Statistical analysis

Statistical analysis was performed by Statistica 8.0, StatSoft (Inc., USA) software to obtain the best operational conditions for the oxidation of NOM. A factorial design in two levels and three variables (2^3) was used to evaluate the effect of the independent variables (initial pH, H_2O_2 dosage, and ZVI nail amount) and their levels on the ZVI/H_2O_2 process (Table A.3). Among such experiments, three were performed at the central point conditions for the estimation of the experimental error. ANOVA test was carried out to assess the difference in significance between data, and a p-value < 0.05 was considered statistically significant.

3. Results and discussion

3.1 Characteristics of the simulated water containing HA and natural water

Although commercial HA has been used as the research matrix in some studies [66,67], it is important to consider the composition differences between commercial HA solutions and natural waters. Such differences result in variation of the efficiency of chemical water treatments applied in these diverse matrices [68]. In this way, the performance of ZVI/H_2O_2 was evaluated to treat simulated water containing commercial HA and real natural water samples collected from the Regent's Park lake. Table 1 shows the characterization of the simulated water ([HA] = 5 mg L^{-1}) and surface water from Regent's Park lake, London.

$SUVA_{254}$ has been used as one of the parameters of better correlation with the organic matter aromaticity and aquatic humic composition [5,66]. The high $SUVA_{254}$ value obtained from the simulated water containing HA (6.2 L mg^{-1} m^{-1}) indicates the presence of higher aromatic carbon content and hydrophobic compounds than in the natural water (2.21 L mg^{-1} m^{-1}). DOC concentration was significantly higher in the natural water, highlighting the variety of possible organic substances present in natural waters, not necessarily with higher hydrophobic compounds.

Consequently, differences in the efficiency of the ZVI/H_2O_2 process were observed. Greater UV_{254} removal in the simulated water containing HA (93.3% ± 0.95) compared to that in natural water (69.9% ± 2.94) can be seen in Figure A.2 (initial pH = 5.5, ZVI nail = 37.5 g L^{-1} and [H_2O_2] = 50% excess of stoichiometric dosage i.e results of the central point from the Statistica software, carried out in trilpicate to verify the experimental error). Considering the higher $SUVA_{254}$ value in the simulated water (Table 1), the higher UV_{254} removal obtained in this sample occurred probably due to the larger number of active sites in its aromatic structure available for reacting with the HO• [21,69–71]. In addition, carbonate and bicarbonate ions are typically present in natural water [44] (From Table 1 conductivity of natural and simulated water are = 1007 ± 39.6 and 37.6 ± 0.1 µs.m^{-1}, respectively). Some HO• radical reacts with carbonate/bicarbonate ions, therefore, the HA removal in natural water may be lower than that in simulated water.

During the first 15 min of ZVI/H_2O_2 reaction in the simulated water containing HA, no changes in UV_{254} were observed, as shown in Figure A.2. This may have been due to the interference of iron ions dissolved in solution, which can absorb ultraviolet light at 253.7 nm [52].

3.2 Effect of initial pH

The influence of initial pH on NOM degradation by the ZVI/H_2O_2 processes applied to Regent's Park water was investigated over the pH range of 4.5–6.5. Figure 1(a) confirms the reduction of DOC when the initial pH was elevated, with 51%, 30% and 8% of removal, corresponding to initial pH 4.5, 5.5 and 6.5, respectively. The same trend was observed for UV_{254} removal (Figure A.3). As shown in Figure 1(b), the ZVI/H_2O_2 applied in a more acidic pH range allowed greater leaching of ferrous ions from the nails. This increased leaching promotes the formation of radicals with sufficient oxidative potential to degrade the organic contaminants [72]. However, when the aqueous solution reaches neutral pH values, the oxidation rate of the process is delayed by the formation of solid iron oxyhydroxides (Equations (1)–(4)), which are weaker activating agents than Fe^{2+}(aq), resulting in decreased rate of production of HO• radicals [22,26,56]. The initial raise followed by the decay of Fe^{2+} concentrations in aqueous medium after 5 min of treatment (at pH 4.5 and 5.5) shown in Figure 1(b) may indicate that there is a fast initial step of Fe dissolution caused by H_2O_2 oxidation according to Equation (1). This would be followed by its (Fe^{2+}) consumption in reaction with H_2O_2 to form radicals with oxidative potential (Equation (2)). In addition to this reaction step, the reduction in the concentration of Fe^{2+} in the

Table 1. Mean and standard deviations of compositional characteristics of the simulated water containing HA (5 mg L^{-1}) and natural water (from Regent's Park).

Parameters	Unit	Simulated water containing HA (n = 3)	Natural water (n = 5)
UV_{254}	cm^{-1}	0.15 ± 0.001	0.144 ± 0.02
* SUVA	L mg^{-1} m^{-1}	6.2	2.21
pH		7.2 ± 0.7	8.0 ± 0.26
*DOC	mg L^{-1}	2.4 ± 0.14	6.52 ± 2.5
Conductivity	µs m^{-1}	37.6 ± 0.1	1007 ± 39.6
Dissolved Oxygen	mg L^{-1}	5.6 ± 0.1 (27 ± 1 °C)	3.5 ± 0.96 (22 ± 1 °C)
Turbidity	NTU	1.03	1.13 ± 0.19
Chlorine (free)	mg L^{-1}	0	0.03 ± 0.01
Chloride	mg L^{-1}	ND	90.7 ± 0.81
Sulphate	mg L^{-1}	ND	141.9 ± 2.3

*SUVA: specific ultraviolet absorbance ($SUVA_\lambda$= UV_λ/DOC, where λ is a specified wavelength). *DOC: dissolved organic carbon. *n = number of samples.
*ND: not detected.

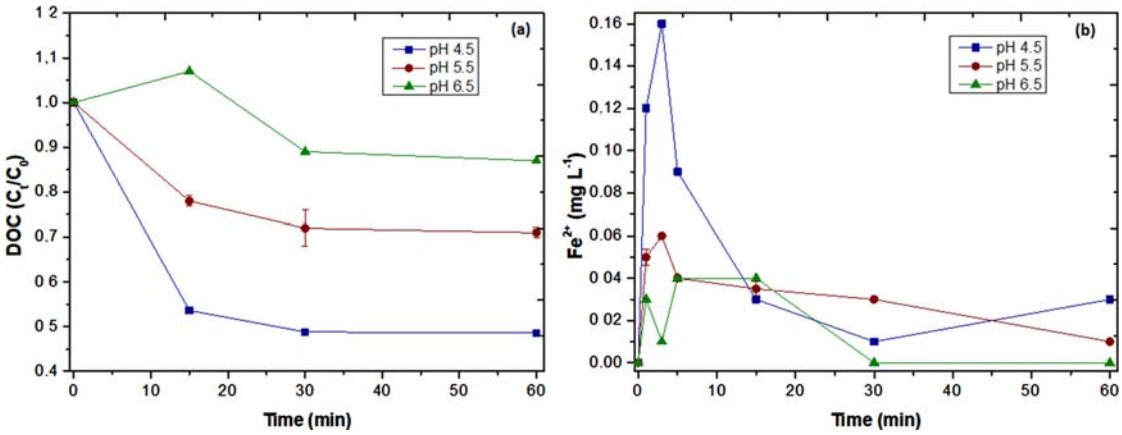

Figure 1. Effect of pH on (a) DOC removal and (b) iron ferrous formation in natural water during the ZVI/H_2O_2 process. Experimental conditions: $pH_0 = 4.5$ ((■)) and 6.5 ((▲)): ZVI nail = 50 g L^{-1} and $[H_2O_2]$ = 100% excess of stoichiometric dosage (85 mg L^{-1}). Experimental conditions from factorial design statistical (central point): $pH_0 = 5.5$ ((●)): ZVI nail = 37.5 g L^{-1} and $[H_2O_2]$ = 50% excess of stoichiometric dosage.

solution can occur due to the formation of solid iron oxyhydroxides (Equation (4)). Previous studies using micro powder ZVI in the ZVI/H_2O_2 process reported attained concentrations of Fe^{2+} (aq) similar to those obtained in this study [32,73].

As the AOP investigated is a step prior to conventional water treatment steps, the remaining iron ions from ZVI/H_2O_2 process can be used as part of the coagulant in the following step of drinking water treatment (coagulation/flocculation). In the present work, it was not possible to measure the total iron concentration and compare the results with the standards for drinking water. However, the total concentration of iron in the final treated water should not be higher than that required by legislation in the final treated water (maximum limit allowed for total [Fe] by Brazilian standard: 0.3 mg L^{-1} [47] and British standard: 0.2 mg L^{-1} [74]).

$$Fe^0 + H_2O_2 + 2H^+ \rightarrow Fe^{2+} + 2H_2O \quad (1)$$

$$Fe^{2+} + H_2O_2 \rightarrow Fe^{3+} + HO\bullet + OH^- \quad (2)$$

$$Fe^{3+} + H_2O_2 \rightarrow Fe^{2+} + HO_2\bullet + H^+ \quad (3)$$

$$Fe^{2+} + \frac{1}{2}H_2O_2 + 2OH^- \rightarrow Fe(OH)_3(s) \quad (4)$$

Figure 2 shows that the pH of the natural water and simulated water containing HA increased during the reaction. This may indicate the kinetic prevalence of H^+ consuming reaction (Equation (1)) together with OH^- generation reaction (Equation (2)) which is known to be much faster than Equation (3). Thus, in the course of the overall reaction, the OH^- consumed in Equation (4) is not enough to compensate and neutralize the H^+ consumption and OH^- generation by the sum of reaction steps (Equation (1)) and (Equation (2)) [26,36,75]. One of the main factors that hinders the applicability of the conventional Fenton process is the need for a subsequent pH adjustment to a higher value (close to neutrality) for the subsequent coagulation/flocculation steps in the WTPs, increasing the process costs [76]. Thus, the proposed ZVI/H_2O_2 process shows the additional advantage of spontaneously increase the pH to a convenient range (6–7.5 in natural water), along the course of the reaction. Consequently, a pH adjustment step using a base for the subsequent coagulation/flocculation steps may not be necessary, reducing treatment costs and process complexity.

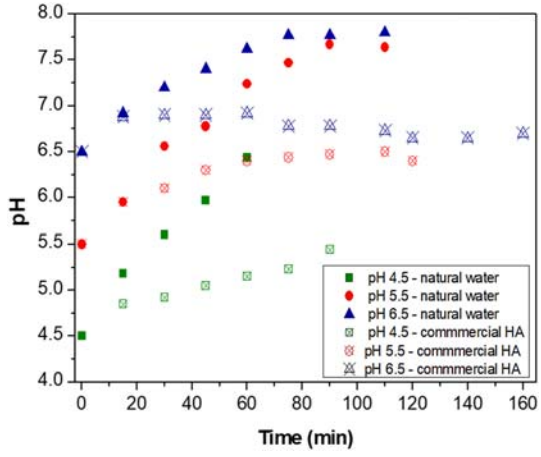

Figure 2. Behavior of pH in simulated water containing HA (commercial HA) and in natural water during the ZVI/H_2O_2 process. Experimental conditions: $pH_0 = 4.5$ (natural water: ■ and commercial HA:⊠) and 6.5 (natural water: ▲ and commercial HA:⊠): ZVI nail = 50 g L^{-1} and $[H_2O_2]$ = 100% excess of stoichiometric dosage. Experimental conditions from factorial design statistical (central point): $pH_0 = 5.5$ (natural water: ● and commercial HA:⊠): ZVI nail = 37.5 g L^{-1} and $[H_2O_2]$ = 50% excess of stoichiometric dosage.

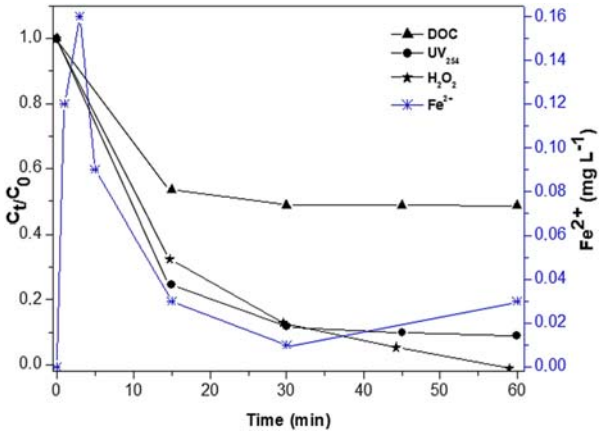

Figure 3. Variation of H_2O_2 (★) and $Fe^{2+}_{(aq)}$ (✳) during the ZVI/H_2O_2 process. NOM removal was evaluated by UV_{254} (●) and DOC (▲) parameters. Experimental conditions: $pH_0 = 4.5$; ZVI nail = 50 g L^{-1}; $[H_2O_2]$ = 100% excess of stoichiometric dosage (85 mg L^{-1}). Initial DOC concentration = 4.9 mg L^{-1}.

The dosages of H_2O_2 and ZVI nail for the NOM degradation runs were applied in two levels: $[H_2O_2]$ = stoichiometric and 100% excess of stoichiometric dosage and ZVI nail = 25 and 50 g L^{-1}. The choice of these values was based on the previous results for HA removal from simulated water containing commercial HA [77]. Figure A.4 shows the removal of DOC and UV_{254} at two different H_2O_2 dosages (43 mg L^{-1} and 85 mg L^{-1}). The results indicated that the higher degradation rates were reached at $[H_2O_2]$ = 100% excess (85 mg L^{-1}), with 51% degradation of DOC and 89% of UV_{254}. This result explains the greater amount of HO• in the reaction medium when the H_2O_2 concentration is high (up to a certain concentration) [78]. In this study, after the H_2O_2 concentration reached <0.5 mg L^{-1}, the possibility of NOM degradation by oxidation was considered to have ceased.

3.3 Effect of H_2O_2 and ZVI nail dosages

The run dosed with 100% excess of H_2O_2 (85 mg L^{-1}) at initial pH 4.5 showed a fast oxidant consumption in the first 15 min of reaction, being about 66% of H_2O_2 consumed ($k = 0.0725$ min^{-1} (Equation (5))). This behaviour may be a consequence of the reaction between the H_2O_2 and H^+ ions with the ZVI nail surface, simultaneously releasing ferrous ions into the solution [79]. Results of Figure 3 shows higher concentration of ferrous ions in aqueous medium at the beginning of the ZVI/H_2O_2 reaction, which provided a higher catalytic effect to the H_2O_2 consumption [44,80]. Consequently, greater removal of DOC and UV_{254} was observed in this time interval. After this time, the rate of HO• generation may have been reduced due to the lower concentration of ferrous ions available to react with H_2O_2, which justifies the lower H_2O_2 consumption ($k = 0.0642$ and 0.0585 min^{-1} for 30 and 45 min, respectively) and reduced DOC removal. The removal of UV_{254} after 15 min (shown in Figure 3) probably occurred from reactions of other iron species with the remaining H_2O_2, which can produce reactive oxygen species with lower oxidative potential, but still sufficient to reduce the humic structures of NOM [44].

The calculations of the pseudo-first order constants of the H_2O_2 concentration decay were performed according to Equation (5) [32,81].

$$\ln([H_2O_2]/[H_2O_2]_0) = -kH_2O_2 . t \quad (5)$$

where kH_2O_2 is the velocity constant for the H_2O_2 decay reaction during the ZVI/H_2O_2 process at a given time.

Evaluating the dosage of 100% excess H_2O_2 in different amounts of ZVI nail applied to the process (pH 4.5), the H_2O_2 consumption at 15 min of the reaction was higher in the ZVI nail amount of 50 g L^{-1} (k = 0.0725 min^{-1}, $R^2 = 0.952$) when compared to the 25 g L^{-1} ZVI nail amount ($k = 0.0243$ min^{-1}, $R^2 = 0.983$). The highest Fe^{2+} concentrations leached to the solution were found mainly during the first minutes of reaction, with 0.012 mg L^{-1} and 0.12 mg L^{-1} (reaction time = 1 min) for ZVI nail = 25 g L^{-1} and ZVI nail = 50 g L^{-1}, respectively. Hence, the DOC removal values reached with ZVI nail = 50 g L^{-1} (51%) were highest than ZVI nail = 25 g L^{-1} (41.3%). Within 60 min of reaction, 99% consumption of H_2O_2 with ZVI nail = 50 g L^{-1} was achieved in contrast to 70.4% with ZVI nail = 25 g L^{-1}.

Considering that only the dissolved ferrous iron concentration was measured in this study, it is suggested for future studies to determine also the dissolved ferric iron concentration, as both species would be present during the process [73].

3.4 Effects of ZVI/H_2O_2 on DOC, UV_{254}, $SUVA_{254}$ and MW

The effects of ZVI/H_2O_2 advanced oxidation on DOC, UV_{254}, $SUVA_{254}$, and MW parameters in the natural water were evaluated from the best experimental condition obtained in this study (pH = 4.5 and H_2O_2 = 100% excess). Statistical tests confirmed the pH and excess of H_2O_2 dosage as variables with a significant influence on DOC mineralization ($R^2 = 0.956$), presenting p-values < 0.05, as shown in Table A.4. In this table, the column 'Effect' results show negative and positive values of the variables, confirming that by decreasing the pH and increasing the dosage of H_2O_2 in the process DOC removals enhanced significantly ($p = 0.024877$ for both pH and excess of H_2O_2 dosage variables).

The partial mineralization of DOC achieved from lower pH level followed by higher H_2O_2 dosage contributed to the expressive reductions of the humic fractions, hydrophobic content, and consequently, molecular weight (indicated by parameters UV_{254}, $SUVA_{254}$, and MW, respectively), as shown in Table A.5. The results show lower DOC mineralization efficiency compared to UV_{254} removal (DOC = 51% and UV_{254} = 89%), corroborating previous AOPs studies for HA removal [5,44,48,69,70]. However, the significant removal of $SUVA_{254}$ (78%) indicates a reduction in hydrophobic carbon content as a loss of aromatic structures and conjugated double bonds presents in NOM [5,44,48,69,70]. It is worth mentioning that because of the reduction of $SUVA_{254}$, it was verified that ZVI/H_2O_2 treatment also favoured the reduction of MW of NOM contained in natural water in 74% (after 60 min of ZVI/H_2O_2 treatment) (Table A.5). The reduction of these medium/micro molecules indicates the conversion of large organic structure into simpler molecules [70]. The initial MW value obtained in this study is similar to what has already been detected in some surface waters for potabilization [82]. These results reinforce that those possible reactions between HO• and NOM (such as HO• radical addition reactions to aromatic sites) may not be sufficient for the full range of mineralization [83], but favour the reduction of the structural complexity of the aromatic fractions of NOM [44].

Additional experimental results are presented in Table A.6, confirming the greater DOC and UV_{254} removals as the pH range is reduced and the H_2O_2 dosages are increased on the ZVI/H_2O_2 process.

3.5. THM formation

In this study, Chloroform ($CHCl_3$) was the only THM species detected before and after the ZVI/H_2O_2 reaction (ZVI nail = 50 g L^{-1}; [H_2O_2] = 100% of excess and initial pH = 4.5 and 6.5) in the chlorinated natural water. The possibility that bromide was converted to bromate in the treated water [84,85], and it was no longer available to be incorporated into the NOM, should be considered with caution. Complementary results (at acidic pH ranges) indicated a low oxidation rate of bromide during the ZVI/H_2O_2 treatment (bromide before ZVI/H_2O_2 = 0.24 mg L^{-1} and bromide after ZVI/H_2O_2 = 0.21 mg L^{-1}). Previous studies have also identified $CHCl_3$ in surface water and wastewater in higher concentrations compared to brominated species [45,48,86,87].

The $CHCl_3$ formation before and after the ZVI/H_2O_2 process are shown in Figure 4, confirming a significant reduction in $CHCl_3$ formation in samples treated at initial pH 4.5. The efficient removal of humic/aromatic structures of the NOM observed within 60 min of the ZVI/H_2O_2 process at pH 4.5 (UV_{254} removal: 89% and 53% to initial pH 4.5 and 6.5, respectively) may explain this reduction of the $CHCl_3$ formation. Previous studies showed that the structure of NOM and of its by-products could determine the concentration of THM formed during the chlorination step [3,87]. After 24 h of Ct, the sample treated with ZVI/H_2O_2 at pH 4.5 showed a 48% reduction in $CHCl_3$ formation compared to the untreated water.

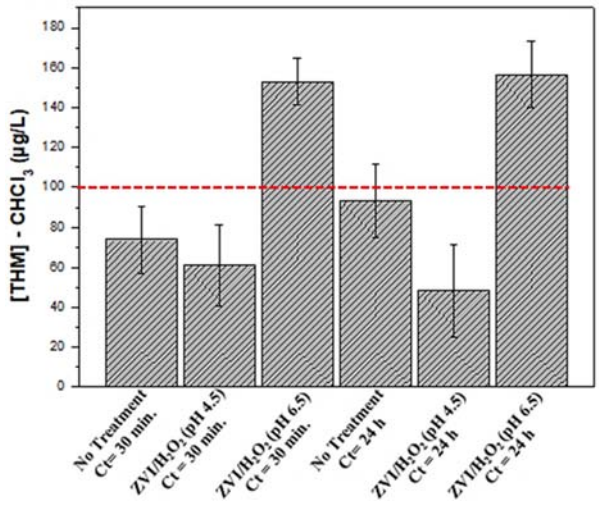

Figure 4. Chloroform ($CHCl_3$) formation before and after ZVI/H_2O_2 treatment at contact times (Ct) of 30 min and 24 h. Experimental conditions ZVI/H_2O_2: ZVI nail = 50 g L^{-1}; [H_2O_2] = 100% excess of stoichiometric dosage and pH 4.5 and 6.5. Sample initial UV_{254}: no ZVI/H_2O_2 treatment = 0.182 ± 0.003 (cm^{-1}), with ZVI/H_2O_2 treatment (pH_0 4.5) = 0.184 ± 0.001 (cm^{-1}) and with ZVI/H_2O_2 treatment (pH_0 6. 5) = 0.180 ± 0.002 (cm^{-1}). Dotted line indicates the maximum limit of [THM_{total}] allowed according to British and Brazilian regulations.

In contrast to the pH 4.5 results, the high concentration of $CHCl_3$ observed after the ZVI/H_2O_2 treatment at initial pH 6.5 (Ct_{24h} = 156.4 ± 20.48 µg L^{-1}) exceeded the maximum values for total THMs allowed for drinking water according to the Brazilian and British standards (< 100 µg L^{-1}) [47,74], as shown in Figure 4 (dotted line). Golea et al. [88] showed a significant correlation (R^2 = 0.82) between the formation of THMs and values of the parameter UV_{254} in surface waters used for drinking water. Other researchers also confirmed that the high $CHCl_3$ formation may be a consequence of the lower efficiency to remove HA [44,89,90]. This high $CHCl_3$ value in samples treated at pH 6.5 in this study may be due to the formation of more chlorine reactive byproducts in addition to the low reduction of the aromatic organic structure observed after AOP ZVI/H_2O_2. However, to prove the influence of these byproducts on the formation of $CHCl_3$, more in-depth study and

analysis of the identification of the formed intermediate species are necessary.

3.6 Characterization of ZVI nail and its corrosion products

The oxidation of ZVI nail used in the ZVI/H_2O_2 process ($pH_0 = 4.5$; $H_2O_2 = 100\%$ of excess and ZVI nail = 50 g L^{-1}) was confirmed by electron microscopy analyses. In addition to chemical results, these analyses provided images of the oxidized surface of the metal and the morphology of its oxides, helping understand the oxidative process. SEM results showed less ZVI nail corrosion on its surface prior to the reaction with H_2O_2, which was supported by the XEDS elemental maps (Figure A.5 (a)). Different characteristics of the ZVI nail surface were observed after the reaction with 100% excess of H_2O_2, confirming the intense surface oxidation of ZVI nail after its reaction with H_2O_2 (and H^+ ions of the solution), producing an uneven rough surface (Figure A.5 (b)). The formation of ferrous ions as a product of ZVI oxidation favour the degradation of organic matter, as these ions are responsible for reacting with H_2O_2 to produce HO• in the Fenton process [31,91,92].

The presence of the oxide species on the surface of the reacted ZVI nail was confirmed by XRD analysis. The identified species were: (1) Iron (Fe) (44.6°, 65° and 82.3°) (2) magnetite (Fe_3O_4) (30.05° 35.4° and 56.9°) and (3) lepidocrocite (γ-FeOOH) (14.16°, 27.08°, 36.5° e 47.05°) (Figure A.6). Previous studies based on water/wastewater treatment applying commercial iron powders also reported the formation and deposition of such species on the surface of the reacted ZVI [32,91–94], as shown in this investigation.

SEM characterization confirmed the complex oxide morphologies on the ZVI nail surface after the oxidative process (Figure 5 (a–d)). The secondary electron image of the oxide in Figure 5(b) exhibited a plate-like or flake-like structure, generally related to the presence of lepidocrocite hydroxide [93,94]. The fine spherical oxides (less than 200 nm) shown in Figure 5(c) are consistent with the morphology of magnetite [95,96]. The oxide morphology shown in Figure 5(d) may be lepidocrocite in a different formation stage when compared to the structure stage shown in Figure 5(b).

XPS analyses shown in Figure A.7 (a,b) confirmed the formation and deposition of oxides/hydroxides on the surface of the ZVI nail. In this figure, ZVI nail O 1s spectrum before reaction with H_2O_2 showed fewer peaks and greater symmetry (peak at 530.7 eV in the O 1s spectrum attributed to Fe-O) [97,98] (Figure A.7 (a)) compared to ZVI nail after reaction with H_2O_2 (Figure A.7 (b)). The surface of the reacted ZVI nail peaked at 531.42 eV, which indicated typical OH^- hydroxide-binding O 1s binding energy [95,96], and energy values at 529.91 eV indicating binding between O and Fe [96].

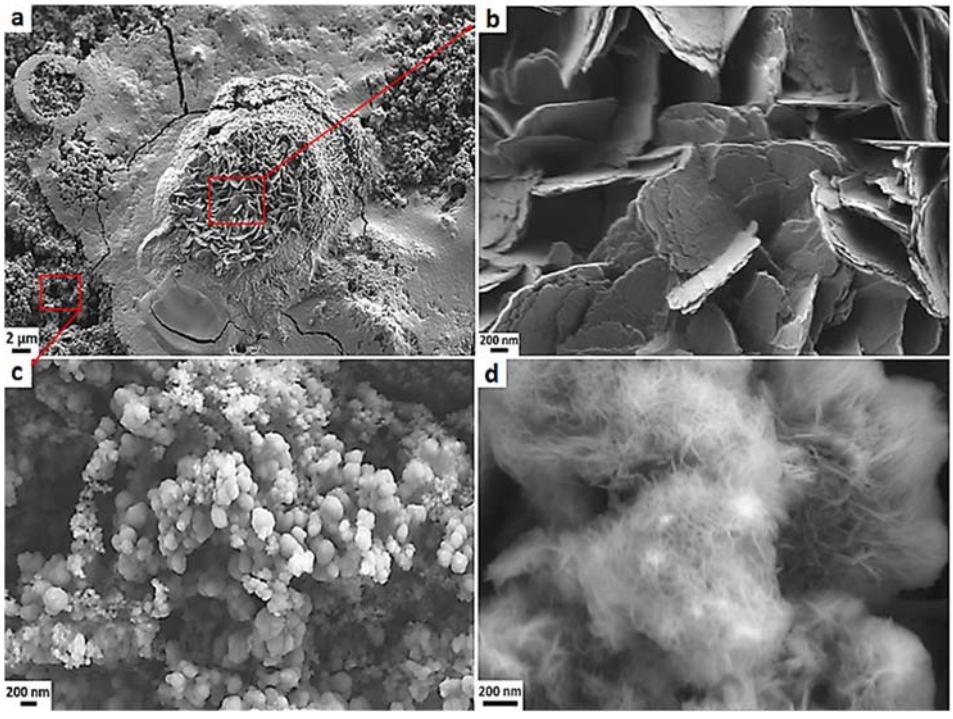

Figure 5. SEM/SE images obtained from the nail-ZVI surface after ZVI/H_2O_2 reaction showing (a) different oxidation product morphologies in the same region, (b) flake-like structure (lepidocrocite), (c) fine spherical oxides (magnetite), and (d) lepidocrocite in a different formation stage. Experimental conditions: $pH_0 = 4.5$, ZVI nail = 50 g L^{-1} and [H_2O_2] = 100% excess of stoichiometric dosage.

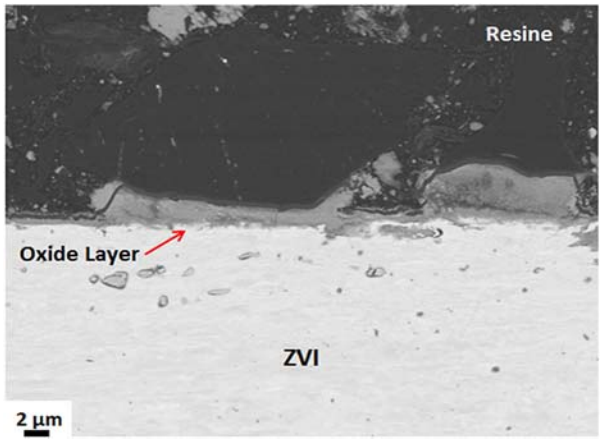

Figure 6. SEM/BSE image of a cross-section nail-ZVI sample showing the passive layer formed during the ZVI/H_2O_2 reaction. Experimental conditions: $pH_0 = 4.5$, ZVI nail = 50 g L^{-1}, and $[H_2O_2]$ = 100% excess of stoichiometric dosage.

The formation of these oxides and hydroxides on the surface of the ZVI plays a critical role in removing contaminants, either by adsorption, precipitation, co-precipitation [99] or by favouring the formation of a passive layer on the metal [94], which limits the mass transport of ferrous ions from ZVI to the aqueous solution [36,100]. The presence of this multi-oxide layer transition-zone was confirmed by SEM/BSE analysis from the ZVI nail cross-section specimen after the ZVI/H_2O_2 reaction (Figure 6). The different contrast in this image is due to the atomic number (compositional) difference between the regions, with the brighter contrast associated with the highest atomic weight (Fe in this figure) [101] and the grey contrast indicative of the oxide layer on the ZVI nail surface.

The presence of these complex oxides on the surface of the ZVI nail formed during the ZVI/H_2O_2 process (verified by SEM, XRD, and XPS analyses) forms the passive layer (identified by SEM/BSE and cross-section analyses), which can limit the mass transport of iron ions from the ZVI nail to the aqueous solution. Thus, it can be speculated that the NOM removal after certain ZVI/H_2O_2 reaction time (as discussed in Section 3.7) might have been influenced by this oxide layer formed.

3.7. Overall remarks about the iron-nails ZVI/ H_2O_2 process

The removal of DOC (51%) and UV_{254} (89%) attained from the application of the ZVI/H_2O_2 process in natural water shown in this investigation indicated an important contribution of this system as a NOM pre-oxidation strategy in water treatment processes.

Experimental results revealed that NOM removal was predominant at the initial time period of the ZVI/H_2O_2 reaction, especially over DOC removal. The AOP applied in this investigation at initial pH 4.5 showed that in 15 min of reaction, the DOC mineralization reached 46% with 66% H_2O_2 consumption (k = 0.0725 min^{-1}). In 30 min of reaction, DOC removal reached 51% with lower H_2O_2 consumption velocity (k = 0.064 min^{-1}) and lower concentration of dissolved Fe^{2+} in the solution (Figure 3). These results suggest that other radicals with lower oxidative redox potential radicals [78,102–104] and other iron species formed in this time interval are factors potentially responsible for the reduction in mineralization rates (Equations (6)–(8)).

$$Fe^0_{(s)} + H_2O_2 + 2H^+ \rightarrow Fe^{2+}_{(aq)} + 2H_2O \quad (6)$$

$$H_2O_2 + Fe^{2+}_{(aq)} \rightarrow Fe^{3+}_{(aq)} + HO\cdot + OH^-(k = 40 - 80M^{-1}s^{-1}) \quad (7)$$

$$H_2O_2 + Fe^{3+}_{(aq)} \rightarrow H^+ + Fe^{2+}_{(aq)} + HO\cdot_2/O\cdot_2^- + H^+(k = 9.0 - 10^{-7}M^{-1}s^{-1}) \quad (8)$$

The greatest DOC removal observed in the initial 15 min of the reaction was referred to as Stage I, as shown in Figure 7 (Fe^0/H_2O_2 and Fe^{2+}/H_2O_2). After this reaction time, they may have overlapped another stage, which is the controlling step of the overall reaction of this process, referred to as Stage II (Figure 7). Then, it could be hypothesized that the results of the ZVI/H_2O_2 experiments (at initial pH 4.5 and 5.5) applied

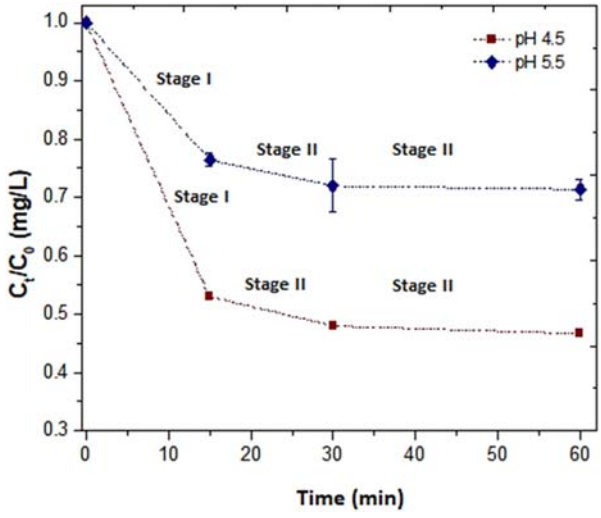

Figure 7. DOC decay during the ZVI/H_2O_2 process applied to Regent's Park lake samples. Experimental conditions: $pH_0 = 4.5$, ZVI nail = 50 g L^{-1} and $[H_2O_2]$ = 100% excess of stoichiometric dosage. Experimental conditions from factorial design statistical (central point): $pH_0 = 5.5$, ZVI nail = 37.5 g L^{-1}, $[H_2O_2]$ = 50% excess of stoichiometric dosage (triplicate experiments).

to Regent's Park lake's water show the presence of these two stages (Figure 7).

The slowing down of the mineralization of the organic content observed in this investigation may be due to the influence of several factors. For example, the pH of the aqueous medium may have also influenced the oxidative process kinetics (as shown in Figure 1). This is because different radical species with lower oxidative potential could have been generated in the system, especially when the pH of the aqueous medium is above 5.0 [92]. This observation explains the lower NOM removal and, consequently, higher Chloroform THM formation, as identified in the ZVI/H_2O_2 experiment at the initial pH 6.5 (Figure 4). Also, the formation and deposition of the oxide/hydroxide layer on the surface of the ZVI nail oxidized identified in this paper (shown in Figures 5 and 6 and Figures A.6–A.7) needs to be investigated, as it may slow down the metal dissolution step [105,106]. The effect and practical implications of this passive layer formation are being investigated and will be discussed in future publications.

It is highlighted that previous investigations with other AOPs, such as O_3/UV, O_3/H_2O_2, UV/H_2O_2, photo-Fenton, and Electrical discharge plasma for NOM and HA removal (as pre-oxidation step or after filtration step) [44,71,87,107,108], showed similar DOC removal in comparison to this paper (applied as a pre-oxidation step, without previous physico–chemical treatment). However, the ZVI/H_2O_2 process investigated here has the advantage of making use of an easily accessible and low-cost reagent (i.e. commercial iron-nails) for the preliminary removal of NOM in drinking water treatment.

In addition to monitoring the NOM, a set of contaminanting elements that may be present in natural and treated waters such as Al, Cd, Cr, and Cu were analysed before and during the ZVI/H_2O_2 process (initial pH 4.5 and 6.5, ZVI = 50 g L^{-1} and H_2O_2 100% excess of stoichiometric dosage). From the experimental conditions applied in this study, the removal of these elements was not observed as shown in Table A.7. At the end of the experiments, Cr, one of the elements present in the composition of the ZVI-nail (Table A.1) presented concentrations close to that found in natural water before ZVI/H_2O_2 treatment. Thus, it is not possible from these results to affirm a Cr leaching effect from the ZVI-nail to the treated water. Also, element concentrations were well bellow drinking water standards (in mg L^{-1}: Al: 0.1; Cd: 0.005; and Cu: 2.0) [47].

The authors propose further studies with nail-ZVI/H_2O_2 in continuous mode to evaluate the iron nails performance. Also, the additional reduction of NOM which is expected to occur in the steps of the conventional treatment train after the ZVI/H_2O_2 pre-oxidation discussed in this paper is an interesting proposal for future investigations on the efficiency of coagulation and quantification of THM formation.

Conclusions

- Two variables had a significant effect ($p < 0.05$) on the mineralization of NOM present in natural water: H_2O_2 concentration (best at 100% of excess) and initial pH (best at 4.5). The NOM removal evaluated by DOC, UV_{254}, $SUVA_{254}$, and MW after ZVI/H_2O_2 treatment in these operating conditions led to lower concentration and lower reactivity of its remaining structure with chlorine, resulting in the best condition, with 48% less formation of THM Chloroform in comparison with no pre-oxidation. The ZVI nails employed in the present study were significantly oxidized by H_2O_2 in the presence of H^+ ions in the solution, confirming their reactivity and capacity of producing aqueous Fe ions with catalytic activity for the Fenton reaction. The formation of different oxide structures on their surface was verified as resulting from oxidative reactions.
- The observed spontaneous increase in pH along the course of the reaction from initial pH 4.5 to the range pH 5.5–6 favours the insertion of this pre-oxidation step in conventional water treatment trains, as this range of final pH after pre-oxidation is typical of surface waters. Fe hydroxide precipitates formed in the water as part of the reaction mechanism can aid the coagulation-flocculation process and can be subsequently incorporated in the sludge removed in the sedimentation stage.
- In addition to these results, the low-cost of commercial iron-nails, their wide accessibility, and the fact that they can be easily separated from the water after the pre-oxidation reaction step or when necessary, make our proposed AOP very attractive as simple pre-treatment for NOM removal in WTPs. This process may be of interest to water utilities with limited financial resources and infrastructure to implement a more sophisticated and costly water advanced pre-oxidation process.

Acknowledgements

The authors acknowledge Dr Liberato Volpe at the Materials Performance Centre, University of Manchester, for assistance with the FEG-SEM/EDX analyses, and Dr John E. Warren at the Department of Materials X-ray Diffraction Suite, University of Manchester, for technical support, advice, assistance and

data analysis. Special thanks to Dr R. G. Palgrave at the Department of Chemistry, University College London, for XPS analyses and technical support. The Royal Parks are acknowledged for authorising the water sampling at the Regent's Park lake.

Disclosure statement

No potential conflict of interest was reported by the author(s).

Funding

Naiara de Oliveira dos Santos acknowledges her doctoral scholarship supported by the Brazilian Agencies: Coordenação de Aperfeiçoamento de Pessoal de Nível Superior (CAPES), Conselho Nacional de Desenvolvimento Científico e Tecnológico (CNPq), and Fundação Carlos Chagas Filho de Amparo à Pesquisa do Estado do Rio de Janeiro (FAPERJ) (DSC10-01/2018).

ORCID

Luiza C. Campos http://orcid.org/0000-0002-2714-7358

References

[1] Uyguner CS, Bekbolet M. Contribution of metal species to the heterogeneous photocatalytic degradation of natural organic matter. Int J Photoenergy. 2007.

[2] Richardson SD, Plewa MJ, Wagner ED, et al. Occurrence, genotoxicity, and carcinogenicity of regulated and emerging disinfection by-products in drinking water: A review and roadmap for research. Mutat Res - Rev Mutat Res. 2007;636:178–242.

[3] Mohd Zainudin F, Abu Hasan H, Sheikh Abdullah SR. An overview of the technology used to remove trihalomethane (THM), trihalomethane precursors, and trihalomethane formation potential (THMFP) from water and wastewater. J Ind Eng Chem [Internet]. 2018;57:1–14. Available from: https://linkinghub.elsevier.com/retrieve/pii/S1226086X17304410.

[4] Krasner SW, Weinberg HS, Richardson SD, et al. Occurrence of a new generation of disinfection byproducts. Environ Sci Technol. 2006;40:7175–7185.

[5] Gumus D, Akbal F. A comparative study of ozonation, iron coated zeolite catalyzed ozonation and granular activated carbon catalyzed ozonation of humic acid. Chemosphere. 2017;174:218–231.

[6] Karanfil T, Krasner SW, Westerhoff P, et al. Disinfection By-products in drinking water: occurrence, formation, Health effects, and control. Karanfil T, Krasner SW, Westerhoff P, et al., editors. Washington, DC: American Chemical Society; 2008.

[7] Jo CH, Dietrich AM, Tanko JM. Simultaneous degradation of disinfection byproducts and earthy-musty odorants by the UV/H2O2 advanced oxidation process. Water Res. 2011;45:2507–2516.

[8] Murray CA, Parsons SA. Removal of NOM from drinking water: Fenton's and photo-Fenton's processes. Chemosphere. 2004;54:1017–1023.

[9] Sillanpää M. (2014). Natural Organic Matter in Water: Characterization and Treatment Methods. Nat. Org. Matter Water Charact. Treat. Methods.

[10] Kim JK, Jang DG, Campos LC, et al. Synergistic removal of humic acid in water by coupling adsorption and photocatalytic degradation using TiO2/coconut shell powder composite. J Nanomater. 2016.

[11] Hamid NAA, Ismail AF, Matsuura T, et al. Morphological and separation performance study of polysulfone/titanium dioxide (PSF/TiO2) ultrafiltration membranes for humic acid removal. Desalination. 2011;273:85–92.

[12] Lowe J, Hossain MM. Application of ultrafiltration membranes for removal of humic acid from drinking water. Desalination. 2008;218:343–354.

[13] Zahoor M. Removal of humic acid from water through adsorption?ultrafiltration hybrid processes. Desalin Water Treat [Internet]. 2014;52:7983–7992. Available from: http://www.tandfonline.com/doi/abs/10.1080/19443994.2013.855885.

[14] Wang G, Hsieh S, Hong C. Destruction of humic acid in water by UV light-catalyzed oxidation with hydrogen peroxide. Water Res [Internet]. 2000;34:3882–3887. Available from: http://linkinghub.elsevier.com/retrieve/pii/S0043135400001202.

[15] Song S, Huang S, Zhang R, et al. Simultaneous removal of U(VI) and humic acid on defective TiO2−x investigated by batch and spectroscopy techniques. Chem Eng J. 2017;325:576–587.

[16] Zhou H, Smith DW. Advanced technologies in water and wastewater treatment. Can J Civ Eng. 2001;28:49–66.

[17] Sillanpää M, Ncibi MC, Matilainen A. Advanced oxidation processes for the removal of natural organic matter from drinking water sources: A comprehensive review. J Environ Manage [Internet]. 2018;208:56–76. Available from: https://linkinghub.elsevier.com/retrieve/pii/S0301479717311714.

[18] Sarathy S, Mohseni M. The fate of natural organic matter during UV/H2O2 advanced oxidation of drinking water. Can J Civ Eng [Internet]. 2009;36:160–169. Available from: http://www.nrcresearchpress.com/doi/10.1139/S08-045.

[19] Toor R, Mohseni M. UV-H2O2 based AOP and its integration with biological activated carbon treatment for DBP reduction in drinking water. Chemosphere [Internet]. 2007;66:2087–2095. Available from: https://linkinghub.elsevier.com/retrieve/pii/S0045653506012525.

[20] Wu Y, Zhou S, Qin F, et al. Modeling the oxidation kinetics of Fenton's process on the degradation of humic acid. J Hazard Mater. 2010;179:533–539.

[21] Molnar JJ, Agbaba JR, Dalmacija BD, et al. A study on the removal of natural organic matter and disinfection byproducts formation potential from groundwater using Fenton's process. J Adv Oxid Technol. 2011;14:54–62.

[22] Jung HJ, Hong JS, Suh JK. A comparison of fenton oxidation and photocatalyst reaction efficiency for humic acid degradation. J Ind Eng Chem. 2013;19:1325–1330.

[23] Aftab B, Shin H-S, Hur J. Exploring the fate and oxidation behaviors of different organic constituents in landfill leachate upon Fenton oxidation processes using EEM-PARAFAC and 2D-COS-FTIR. J Hazard Mater [Internet]. 2018;354:33–41. Available from: https://linkinghub.elsevier.com/retrieve/pii/S0304389418303091.

[24] Sanly, Lim M, Chiang K, et al. A study on the removal of humic acid using advanced oxidation processes. Sep Sci Technol [Internet]. 2007;42:1391–1404. Available from: http://www.tandfonline.com/doi/abs/10.1080/01496390701289799.

[25] Trellu C, Péchaud Y, Oturan N, et al. Comparative study on the removal of humic acids from drinking water by anodic oxidation and electro-Fenton processes: mineralization efficiency and modelling. Appl Catal B Environ [Internet]. 2016;194:32–41. Available from: https://linkinghub.elsevier.com/retrieve/pii/S0926337316303058.

[26] Santos-Juanes L, García-Ballesteros S, Vercher RF, et al. Commercial steel wool used for zero valent iron and as a source of dissolved iron in a combined red-ox process for pentachlorophenol degradation in tap water. Catal Today. 2019;328:252–258.

[27] Ju Y, Yu Y, Wang X, et al. Environmental application of millimetre-scale sponge iron (s-Fe 0) particles (IV): New insights into visible light photo-Fenton-like process with optimum dosage of H 2 O 2 and RhB photosensitizers. J Hazard Mater [Internet]. 2017;323:611–620. Available from: https://linkinghub.elsevier.com/retrieve/pii/S030438941630886X.

[28] Kallel M, Belaid C, Boussahel R, et al. Olive mill wastewater degradation by Fenton oxidation with zero-valent iron and hydrogen peroxide. J Hazard Mater. 2009;163:550–554.

[29] Babuponnusami A, Muthukumar K. A review on Fenton and improvements to the Fenton process for wastewater treatment. J Environ Chem Eng. 2014;2:557–572.

[30] Teixeira LAC, Vieira NDA, Yokoyama L, et al. Degradation of phenol in mine waters using hydrogen peroxide and commercial steel wool. Int J Miner Process. 2015;138:15–19.

[31] Fu F, Dionysiou DD, Liu H. The use of zero-valent iron for groundwater remediation and wastewater treatment: A review. J Hazard Mater [Internet]. 2014;267:194–205. Available from: https://linkinghub.elsevier.com/retrieve/pii/S0304389413009941.

[32] Ling R, Chen JP, Shao J, et al. Degradation of organic compounds during the corrosion of ZVI by hydrogen peroxide at neutral pH: kinetics, mechanisms and effect of corrosion promoting and inhibiting ions. Water Res. 2018;134:44–53.

[33] Chen Y, Lin J, Chen Z. Remediation of water contaminated with diesel oil using a coupled process: biological degradation followed by heterogeneous fenton-like oxidation. Chemeosphere. 2017;183:286–293.

[34] Santos-Juanes L, García Einschlag FS, Amat AM, et al. Combining ZVI reduction with photo-Fenton process for the removal of persistent pollutants. Chem Eng J. 2017;310:484–490.

[35] Santos N, Spadotto J, Burke M, et al. Removal of humic acid from natural water by ZVI/H 2 O 2 process. Microsc Microanal. 2019;25:798–799.

[36] Segura Y, Martínez F, Melero JA. Effective pharmaceutical wastewater degradation by Fenton oxidation with zero-valent iron. Appl Catal B Environ. 2013;136–137:64–69.

[37] Sigma-Aldrich. Iron Powder - Sigma-Aldrich USA [Internet]. (2020). p. 1–6. Available from: https://www.sigmaaldrich.com/catalog/search?term=iron+powder&interface=All&N=0&mode=matchpartialmax&lang = en &region = US&focus = product.

[38] Chiew H, Sampson ML, Huch S, et al. Effect of groundwater iron and Phosphate on the efficacy of arsenic removal by iron-amended BioSand filters. Environ Sci Technol [Internet]. 2009;43:8698–8698. Available from: https://pubs.acs.org/doi/10.1021/es902520n.

[39] Van Den Bergh K, Du Laing G, Montoya JC, et al. Arsenic in drinking water wells on the bolivian high plain: Field monitoring and effect of salinity on removal efficiency of iron-oxides-containing filters. J Environ Sci Heal Part A [Internet]. 2010;45:1741–1749. Available from: http://www.tandfonline.com/doi/abs/10.1080/10934529.2010.513262.

[40] Bretzler A, Nikiema J, Lalanne F, et al. Arsenic removal with zero-valent iron filters in Burkina Faso: Field and laboratory insights. Sci Total Environ [Internet]. 2020;737:139466. Available from: https://linkinghub.elsevier.com/retrieve/pii/S0048969720329831.

[41] Mueller B, Dangol B, Ngai TKK, et al. Kanchan arsenic filters in the lowlands of Nepal: mode of operation, arsenic removal, and future improvements. Environ Geochem Health [Internet]. 2020;9. Available from: http://link.springer.com/10.1007/s10653-020-00718-9.

[42] Nanseu-Njiki CP, Tchamango SR, Ngom PC, et al. Mercury(II) removal from water by electrocoagulation using aluminium and iron electrodes. J Hazard Mater [Internet]. 2009;168:1430–1436. Available from: https://linkinghub.elsevier.com/retrieve/pii/S0304389409004270.

[43] João JJ, Silva CS da, Vieira JL, et al. Treatment of swine wastewater using the Fenton process with ultrasound and recycled iron. Ambient e Agua - An Interdiscip J Appl Sci [Internet]. 2020;15:1–11. Available from: https://www.scielo.br/scielo.php?script=sci_arttext&pid=S1980-993X2020000300301&lng=en&nrm=iso&tlng=en.

[44] Lamsal R, Walsh ME, Gagnon GA. Comparison of advanced oxidation processes for the removal of natural organic matter. Water Res [Internet]. 2011;45:3263–3269. Available from: https://linkinghub.elsevier.com/retrieve/pii/S0043135411001564.

[45] Wei M-C, Wang K, Hsiao T-E, et al. Effects of UV irradiation on humic acid removal by ozonation, Fenton and Fe0/air treatment: THMFP and biotoxicity evaluation. J Hazard Mater [Internet]. 2011;195:324–331. Available from: https://linkinghub.elsevier.com/retrieve/pii/S0304389411010624.

[46] Liu W, Andrews SA, Stefan MI, et al. Optimal methods for quenching H2O2 residuals prior to UFC testing. Water Res. 2003;37:3697–3703.

[47] Ministério da Saúde. Portaria de Consolidação 5/2017. Brazil; 2017 p. 1–444.

[48] Sarathy S, Mohseni M. Effects of UV/H2O2 advanced oxidation on chemical characteristics and chlorine reactivity of surface water natural organic matter. Water Res [Internet]. 2010;44:4087–4096. Available from: https://linkinghub.elsevier.com/retrieve/pii/S0043135410003337.

[49] EPA (Ireland). (2011). Water Treatment Manual : Disinfection Environmental Protection Agency.

[50] USEPA. (1995). Method 551.1. Chlorinated Solvents, and Halogenated Pesticides / Herbicides in Drinking Water by Liquid-Liquid Extraction and Gas Chromatography with Electro-Capture Deyection. Ohio.

[51] USEPA. (2009). Method 415.3. Determination of Total Organic Carbon and Specific UV Absorbance at 254 nm in Source Water and Drinking Water. Ohio.
[52] Standard Methods. Method 5910. (2011). UV-Absorbing Organic Constituents. Ultraviolet Absorption Method [Internet]. Available from: www.standardmethods.org.
[53] Liu X, Fitzpatrick CSB. Removal of humic substances using solar irradiation followed by granular activated carbon adsorption. Water Sci Technol Water Supply. 2010;10:15–22.
[54] Zhou Q, Cabaniss SE, Maurice PA. Considerations in the use of high-pressure size exclusion chromatography (HPSEC) for determining molecular weights of aquatic humic substances. Water Res. 2000;34:3505–3514.
[55] Sarathy SR, Mohseni M. The Impact of UV/H 2 O 2 advanced oxidation on molecular size distribution of chromophoric natural organic matter. Environ Sci Technol [Internet]. 2007;41:8315–8320. Available from: https://pubs.acs.org/doi/10.1021/es071602m.
[56] Kim JK, Alajmy J, Borges AC, et al. Degradation of humic acid by photocatalytic reaction using nano-sized ZnO/laponite composite (NZLC). Water Air Soil Pollut. 2013;224.
[57] Szabo HM, Tuhkanen T. The application of HPLC–SEC for the simultaneous characterization of NOM and nitrate in well waters. Chemosphere [Internet]. 2010;80:779–786. Available from: https://linkinghub.elsevier.com/retrieve/pii/S0045653510005485.
[58] McBeath ST, Mohseni M, Wilkinson DP. Pilot-scale iron electrocoagulation treatment for natural organic matter removal. Environ Technol [Internet]. 2018;41:577–585. Available from: https://www.tandfonline.com/doi/full/10.1080/09593330.2018.1505965.
[59] McAdams BC, Aiken GR, McKnight DM, et al. High pressure size exclusion chromatography (HPSEC) determination of dissolved organic matter molecular weight revisited: accounting for changes in stationary phases, Analytical Standards, and Isolation Methods. Environ Sci Technol [Internet]. 2018;52:722–730. Available from: https://pubs.acs.org/doi/10.1021/acs.est.7b04401.
[60] Piccolo PC, Cozzolino A. Differences in high perfomance size exclusion chromatography between humic substances and macromolecular polymers. In: Ghabbour EA, Davies G, editor. Humic subst versatile components plants, soils water. Boston: Woodhead Publishing; 2000. p. 111–124.
[61] Rasheed S, Hashmi I, Kim JK, et al. Species-specific interaction of trihalomethane (THM) precursors in a scaled-up distribution network using response surface methodology (RSM). Environ Technol [Internet]. 2018;39:346–355. Available from: https://www.tandfonline.com/doi/full/10.1080/09593330.2017.1301564.
[62] Favoretto E. (2015). EFLUENTES E ÁGUAS DIVERSAS. RESIDUAL DE H2O2 - LA0-MA-057/15 (v. 2.0). Curitiba, Paraná.
[63] Vicente F, Rosas JM, Santos A, et al. Improvement soil remediation by using stabilizers and chelating agents in a fenton-like process. Chem Eng J [Internet]. 2011;172:689–697. Available from: https://linkinghub.elsevier.com/retrieve/pii/S1385894711007492.
[64] Romero A, Santos A, Vicente F. Chemical oxidation of 2,4-dimethylphenol in soil by heterogeneous Fenton process. J Hazard Mater [Internet]. 2009;162:785–790. Available from: https://linkinghub.elsevier.com/retrieve/pii/S0304389408007954.
[65] HACH. HACH DR/890 Procedures Manual. HACH Company; 2013. p. 7–613.
[66] Rodríguez FJ, Schlenger P, García-Valverde M. Monitoring changes in the structure and properties of humic substances following ozonation using UV-Vis, FTIR and 1H NMR techniques. Sci Total Environ. 2016;541:623–637.
[67] Artifon V, Zanardi-Lamardo E, Fillmann G. Aquatic organic matter: classification and interaction with organic micro-contaminants. Sci Total Environ [Internet]. 2019;649:1620–1635. Available from: https://linkinghub.elsevier.com/retrieve/pii/S0048969718333564.
[68] Rodríguez FJ, Schlenger P, García-Valverde M. A comprehensive structural evaluation of humic substances using several fluorescence techniques before and after ozonation. part I: structural characterization of humic substances. Sci Total Environ. 2014;476–477:718–730.
[69] Wang N, Zheng T, Zhang G, et al. A review on fenton-like processes for organic wastewater treatment. J Environ Chem Eng. 2016;4:762–787.
[70] Zhong X, Cui C, Yu S. Identification of oxidation intermediates in humic acid oxidation. Ozone Sci Eng. 2018;40:93–104.
[71] Cui Y, Yu J, Su M, et al. Humic acid removal by gas-liquid interface discharge plasma: performance, mechanism and comparison to ozonation. Environ Sci Water Res Technol. 2019;5:152–160.
[72] Pignatello JJ, Oliveros E, MacKay A. Advanced oxidation processes for organic contaminant destruction based on the Fenton reaction and related chemistry. Crit Rev Environ Sci Technol. 2006;36:1–84.
[73] Wu Y, Fan L, Hu S, et al. Role of dissolved iron ions in nanoparticulate zero-valent iron/H2O2 fenton-like system. Int J Environ Sci Technol [Internet]. 2018;16:4551–4562. Available from: http://link.springer.com/10.1007/s13762-018-2094-z.
[74] Water Supply Regulation. The Water Supply (Water Quality) Regulations 2016 SI No. 614. Regulation 5 [Internet]. SI No. 614 UK; 2016. Available from: http://www.dwi.gov.uk/stakeholders/legislation/.
[75] da Silva MRA, Rodrigues E de O, Espanhol-Soares M, et al. Application of Fenton process to remove organic matter and PCBs from waste (fuller's earth) contaminated with insulating oil. Environ Technol [Internet]. 2019;40:1298–1305. Available from: https://www.tandfonline.com/doi/full/10.1080/09593330.2017.1420699.
[76] Fischbacher A, Sonntag Cv, Schmidt TC. Hydroxyl radical yields in the Fenton process under various pH, ligand concentrations and hydrogen peroxide/Fe(II) ratios. Chemosphere. 2017;182:738–744.
[77] Santos NdOd. Estudo do Processo Oxidativo Avançado FZV / H 2 O 2 para a pré-oxidação da matéria orgânica natural em águas de superfície. PUC RIO; 2019.
[78] Huang Z, Gu Z, Wang Y, et al. Improved oxidation of refractory organics in concentrated leachate by a Fe2+-enhanced O3/H2O2 process. Environ Sci Pollut Res. 2019.

[79] Zhou T, Li Y, Ji J, et al. Oxidation of 4-chlorophenol in a heterogeneous zero valent iron/H2O2 fenton-like system: kinetic, pathway and effect factors. Sep Purif Technol. 2008;62:551–558.
[80] Wu Y, Zhou S, Ye X, et al. Oxidation and coagulation removal of humic acid using Fenton process. Colloids Surfaces A Physicochem Eng Asp. 2011;379:151–156.
[81] Cabrera Reina A, Santos-Juanes Jordá L, García Sánchez JL, et al. Modelling photo-Fenton process for organic matter mineralization, hydrogen peroxide consumption and dissolved oxygen evolution. Appl Catal B Environ. 2012;119–120:132–138.
[82] Zhang Y, Zhang N, Zhao P, et al. Characteristics of molecular weight distribution of dissolved organic matter in bromide-containing water and disinfection by-product formation properties during treatment processes. J Environ Sci. 2018;65:179–189.
[83] Katsumata H, Sada M, Kaneco S, et al. Humic acid degradation in aqueous solution by the photo-Fenton process. Chem Eng J. 2008;137:225–230.
[84] Allard S, Nottle CE, Chan A, et al. Ozonation of iodide-containing waters: selective oxidation of iodide to iodate with simultaneous minimization of bromate and I-THMs. Water Res [Internet]. 2013;47:1953–1960. Available from: https://linkinghub.elsevier.com/retrieve/pii/S004313541200869X.
[85] Liu C, Croué J-P. Formation of bromate and Halogenated disinfection byproducts during chlorination of bromide-containing waters in the presence of dissolved organic matter and CuO. Environ Sci Technol [Internet]. 2016;50:135–144. Available from: https://pubs.acs.org/doi/10.1021/acs.est.5b03266.
[86] Han Q, Yan H, Zhang F, et al. Trihalomethanes (THMs) precursor fractions removal by coagulation and adsorption for bio-treated municipal wastewater: molecular weight, hydrophobicity/hydrophily and fluorescence. J Hazard Mater. 2015;297:119–126.
[87] Sarathy SR, Stefan MI, Royce A, et al. Pilot-scale UV/H 2 O 2 advanced oxidation process for surface water treatment and downstream biological treatment: effects on natural organic matter characteristics and DBP formation potential. Environ Technol [Internet]. 2011;32:1709–1718. Available from: http://www.tandfonline.com/doi/abs/10.1080/09593330.2011.553843.
[88] Golea DM, Upton A, Jarvis P, et al. THM and HAA formation from NOM in raw and treated surface waters. Water Res. 2017;112:226–235.
[89] Valdivia-Garcia M, Weir P, Frogbrook Z, et al. Climatic, geographic and operational determinants of Trihalomethanes (THMs) in drinking water systems. Sci Rep. 2016;6:1–12.
[90] Tungsudjawong K, Leungprasert S, Peansawang P. Investigation of humic acids concentration in different seasons in a raw water canal, Bangkok. Thailand. Water Sci Technol Water Supply. 2018;18:1727–1738.
[91] Sun F, Osseo-Asare KA, Chen Y, et al. Reduction of As(V) to As(III) by commercial ZVI or As(0) with acid-treated ZVI. J Hazard Mater. 2011;196:311–317.
[92] Xu L, Wang J. A heterogeneous fenton-like system with nanoparticulate zero-valent iron for removal of 4-chloro-3-methyl phenol. J Hazard Mater. 2011;186:256–264.
[93] Minella M, Sappa E, Hanna K, et al. Considerable Fenton and photo-Fenton reactivity of passivated zero-valent iron. RSC Adv. 2016;6:86752–86761.
[94] Xiang W, Zhang B, Zhou T, et al. An insight in magnetic field enhanced zero-valent iron/H2O2 fenton-like systems: critical role and evolution of the pristine iron oxides layer. Sci Rep. 2016;6:1–11.
[95] Cai MQ, Zhu YZ, Wei ZS, et al. Rapid decolorization of dye orange G by microwave enhanced fenton-like reaction with delafossite-type CuFeO2. Sci Total Environ. 2017;580:966–973.
[96] Sleiman N, Deluchat V, Wazne M, et al. Phosphate removal from aqueous solutions using zero valent iron (ZVI): influence of solution composition and ZVI aging. Colloids Surfaces A Physicochem Eng Asp. 2017;514:1–10.
[97] Ma Q, Cui L, Zhou S, et al. Iron nanoparticles in situ encapsulated in lignin-derived hydrochar as an effective catalyst for phenol removal. Environ Sci Pollut Res [Internet]. 2018;25:20833–20840. Available from: http://link.springer.com/10.1007/s11356-018-2285-7.
[98] Zhang M, Li J, Wang Y, et al. Impacts of different biochar types on the anaerobic digestion of sewage sludge. RSC Adv [Internet]. 2019;9:42375–42386. Available from: http://xlink.rsc.org/?DOI=C9RA08700A.
[99] Guo X, Yang Z, Dong H, et al. Simple combination of oxidants with zero-valent-iron (ZVI) achieved very rapid and highly efficient removal of heavy metals from water. Water Res. 2016;88:671–680.
[100] Dong J, Zhao Y, Zhao R, et al. Effects of pH and particle size on kinetics of nitrobenzene reduction by zero-valent iron. J Environ Sci. 2010;22:1741–1747.
[101] Goldstein J, Newbury D, Joy D, et al. Scanning electron microscopy and X-ray microanalysis. 3rd ed., Springer, editor. Springer; 2003.
[102] Malik PK, Saha SK. Oxidation of direct dyes with hydrogen peroxide using ferrous ion as catalyst. Sep Purif Technol. 2003;31:241–250.
[103] Bogacki J, Marcinowski P, Zapałowska E, et al. Cosmetic wastewater treatment by the ZVI/H2O2 process. Environ Technol (United Kingdom). 2017;38:2589–2600.
[104] Ifelebuegu AO, Ukpebor J, Nzeribe-Nwedo B. Mechanistic evaluation and reaction pathway of UV photo-assisted fenton-like degradation of progesterone in water and wastewater. Int J Environ Sci Technol. 2016;13:2757–2766.
[105] Landolt D. Corrosion and surface Chemistry of metals. 1st ed., EPFL Press, editor. Lausanne; 2007.
[106] Martins RC, Lopes DV, Quina MJ, et al. Treatment improvement of urban landfill leachates by fenton-like process using ZVI. Chem Eng J. 2012;192:219–225.
[107] Moncayo-Lasso A, Rincon AG, Pulgarin C, et al. Significant decrease of THMs generated during chlorination of river water by previous photo-Fenton treatment at near neutral pH. J Photochem Photobiol A Chem. 2012;229:46–52.
[108] Black KE, Bérubé PR. Rate and extent NOM removal during oxidation and biofiltration. Water Res [Internet]. 2014;52:40–50. Available from: https://linkinghub.elsevier.com/retrieve/pii/S0043135413010166.